Generation of high-repetition-rate femtosecond pulses from 8 to 18 μm

James M. Fraser, Diankui Wang, Alain Haché, Gary R. Allan, and Henry M. van Driel

We generated subpicosecond pulses from 8 to 18 μm by difference-frequency mixing in a 1-mm-thick $AgGaSe_2$ crystal, the 130- and 180-fs output pulses ($1.45 < \lambda < 1.85$ μm) from an 84-MHz-repetition-rate optical parametric oscillator. Numerical simulations show that intrapulse and interpulse group velocity dispersion determine minimum pulse duration above and below 15 μm, respectively. By cross correlation (upconversion) of 10.5-μm pulses with 90-fs, 810-nm pulses in $AgGaS_2$, the pulse length was measured to be 310 fs in good agreement with simulations. © 1997 Optical Society of America

1. Introduction

Femtosecond optical pulses have helped provide considerable insight into ultrafast phenomena in atoms, molecules, and solids. With the advent of the Kerr-lens mode-locked Ti:sapphire laser, production of 10–100-fs pulses has become relatively common, and the high repetition rate (typically approaching 100 MHz) allows for high data acquisition rates and signal averaging. This source, although tunable, is limited to a wavelength range of $690 < \lambda < 1020$ nm. Parametric oscillators and generators pumped by Ti:sapphire lasers can be used to extend this tuning range. For example, synchronously pumped optical parametric oscillators (OPOs) now nominally produce 100-fs pulses in the wavelength region from 1 to 5 μm,[1–4] whereas single-pass, difference-frequency (DF) mixing in $LiIO_3$ or $AgGaS_2$ crystals has provided subpicosecond pulses between 2.5 and 12.5 μm.[5–7] Here we report an extension of the wavelength range of high-repetition-rate femtosecond sources to 18 μm by DF conversion in $AgGaSe_2$, which has a transparency range of 0.8–18 μm and a nonlinear susceptibility[8] ($d_{36} = 37 \pm 6$ pm/V) approximately 50% higher than that[9] of $AgGaS_2$. With a 1-mm-thick crystal and <180-fs input pulses, we obtain DF pulses that are shown to be as short as 300 fs with a cross-correlation technique, corresponding to a few optical cycles. We examine the main limitations to DF-femtosecond pulse generation at these long wavelengths and show that interpulse and intrapulse group velocity dispersion (GVD) determine the minimum pulse duration at different DF wavelengths.

2. Experiment

Figure 1 shows the experimental configuration we used for producing mid-IR femtosecond pulses. We generated these pulses by mixing signal and idler pulses from a critically phase-matched OPO based on potassium titanyl phosphate. The singly resonant OPO is synchronously pumped by 90-fs, 810-nm pulses from an 84-MHz-repetition rate, Kerr-lens mode-locked Ti:sapphire laser with an average output power of 700 mW.[1] With a single mirror set, the OPO yields approximately 80 mW of average power in both signal ($1.45 < \lambda < 1.62$-μm, 130-fs-pulse-width) and idler ($1.62 < \lambda < 1.85$-μm, 180-fs-pulse-width) beams. The signal beam has a near-Gaussian spatial profile whereas the idler beam's profile is elliptical with an aspect ratio of 2:1 because of the angle tuning used. Both beams are collimated, temporally overlapped, and focused by an uncoated 5-cm-focal-length lens onto an uncoated $5 \times 5 \times 1\text{-mm}^3$ $AgGaSe_2$ crystal. For an estimated spot diameter of 100 μm, the average irradiance on the crystal is $<2\ \text{kW cm}^{-2}$, which is well below the level associated with beam degradation caused by thermal lensing effects.[10] The crystal is cut at 66^0 relative to the optic axis and is used in a type-II phase-matching configuration ($e + o \Rightarrow e$; $d_{eoe} = d_{36} \sin 2\theta$ with θ as the internal angle between the input beams and the optic axis). The signal and idler beams are filtered by a germanium slab. Output radiation is produced between 8 and 18 μm and detected with a liquid-nitrogen-cooled HgCdTe detector.

The authors are with the Department of Physics, University of Toronto and Ontario Laser and Lightwave Research Centre, Toronto, Ontario M5S 1A7, Canada.

Received 20 September 1996; revised manuscript received 13 January 1997.
0003-6935/97/215044-04$10.00/0

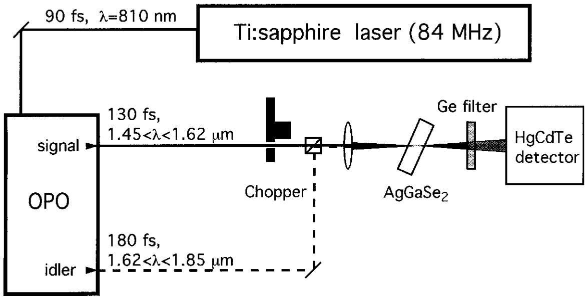

Fig. 1. Experimental setup with FWHM of pulses and tuning ranges indicated. The DF spectra were recorded by replacing the Ge filter with a lens and a monochromator.

Pulse spectra are analyzed with a monochromator with a 200-lines/mm grating blazed for 12 μm.

3. Results and Discussion

Figure 2(a) shows typical spectra of OPO signal and idler pulses that have FWHM bandwidths of 170 and 100 cm^{-1}, respectively. The corresponding time–bandwidth products are 0.67 and 0.54, indicating the presence of chirp in the output pulses from the uncompensated OPO. Mixing of signal and idler pulses for different peak wavelengths under optimum phase-matching conditions yields variable wavelength DF pulses with spectra that are shown in Fig. 2(b). The DF-generated bandwidth is typically 80 cm^{-1}, which is much less than the total available for the mixing process ($100 + 170\ cm^{-1}$). The reduction reflects incomplete phase matching over the entire input bandwidth mainly because of GVD[11] and is consistent with numerical simulations based on the linear optical properties of the crystal.[12]

Analysis of the temporal characteristics of the DF pulse requires some care. The DF pulse width is influenced by the input pulse widths, interpulse dispersion [in the form of group velocity mismatch (GVM) between signal, idler, and DF pulses], and intrapulse GVD within the pulses. Using the linear optical properties of the crystal, we numerically simulated the DF mixing process assuming the slowly varying envelope approximation, negligible pump depletion, and Gaussian input pulse profiles. Given the ~1-cm^{-1} gain coefficient for the downconversion process, the slowly varying envelope approximation is reasonable. Figure 3 shows the calculated DF pulse width as a function of wavelength. For illustration purposes we also show the pulse broadening per millimeter associated with GVD for a pulse with a bandwidth of 80 cm^{-1} and a temporal walkoff per millimeter caused by GVM between the DF pulse and the overlapped signal and idler pulses. Below 15 μm the pulse duration is determined primarily by GVM or temporal walkoff of the DF pulses from the signal and idler pulses, which travel at nearly the same velocity. Beyond 15 μm the pulse spreading caused by GVD dominates, with GVM again playing a minor role at the edge of the transparency range.

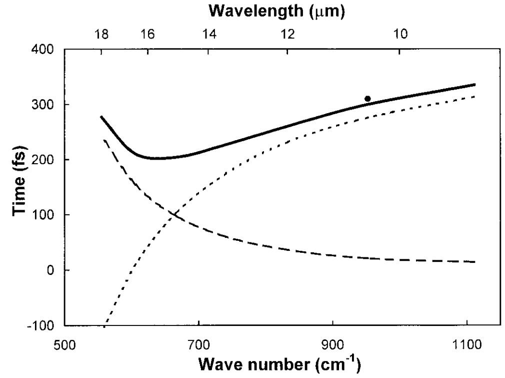

Fig. 3. Calculated DF pulse duration resulting from dispersion effects in $AgGaSe_2$. The dashed curve represents pulse broadening per millimeter associated with GVD for a pulse with a bandwidth of 80 cm^{-1}. The dotted curve represents the temporal walkoff per millimeter caused by GVM between the DF pulse and the overlapped signal and idler pulses. The solid curve represents the calculated DF pulse width as determined by simulations of DF pulse generation from 130- and 180-fs input pulses, mixed in a 1-mm-thick crystal and taking into account GVM and GVD. The data point (●) corresponds to the cross-correlation result, as indicated in Fig. 4.

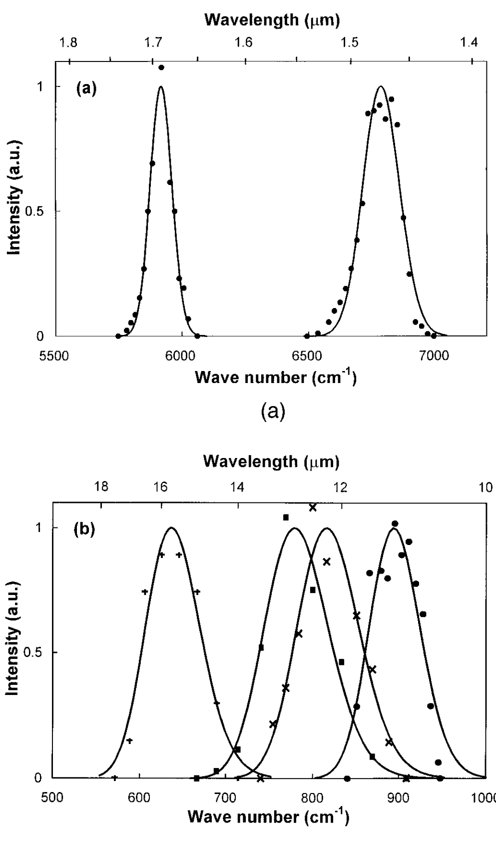

Fig. 2. (a) Normalized spectra of the idler (left trace) and signal beams produced by the OPO. (b) Normalized spectra of the DF beams obtained by tuning the OPO and adjusting the $AgGaSe_2$ phase-matching angle (50°–60°). The lowest wavelength spectrum shown corresponds to the DF beam produced by mixing the signal and idler beams indicated in (a). The solid curves are Gaussian fits.

For wavelengths in which both GVD and GVM are significant, the DF pulse is expected to be asymmetric even for symmetric signal and idler pulse envelopes. Since the DF pulse travels more slowly than either the signal or idler pulses, the leading edge of the pulse rises more rapidly than the falling edge.[13]

To determine the duration of a DF pulse, we measured the cross correlation between 10.5-μm and 810-nm pulses in a $7 \times 7 \times 1\text{-mm}^3$ $AgGaS_2$ crystal, generating 750-nm light with upconversion. The use of this crystal restricted our pulse-width measurement to DF wavelengths below its absorption edge (11.5 μm), so 10.5 μm was the longest center wavelength that could be employed to allow the full pulse spectrum to be transmitted with minimum absorption. The crystal was cut with its optic axis at 45° to the normal input and was used in a type-II phase-matching ($e + o \Rightarrow e$) configuration. Because the upconverted signal was weak, a 750-nm blocking filter was placed in the 810-nm beam, lengthening these pulses to 100 fs. Two interference filters (centered at 750 nm) were also used after the $AgGaS_2$ crystal to suppress the strong background radiation. Detection was accomplished with a photomultiplier tube (Hamamatsu R928) together with lock-in amplification. GVM effects cannot be avoided in these cross-correlation experiments. For a 250-fs DF pulse and a 100-fs near-IR pulse, limiting the temporal walkoff contribution to less than 10% of the FWHM of the cross correlation would require a crystal thickness of <35 μm (Ref. 9), which is too small to permit a measurable signal. The cross-correlation signal between 10.5-μm and 810-nm pulses is shown in Fig. 3. Simply deconvolving the pump pulse width from this trace without taking into account GVM, as was done previously,[5] does not yield the DF pulse width. The 700-fs FWHM mainly reflects the temporal walkoff of the two input pulses. Although this FWHM sets an upper limit on the DF pulse width, information contained in the shape of the cross-correlation refines that upper limit. By numerically modeling the upconversion process, taking into account the 100-fs FWHM of the 810-nm pulse (with assumed Gaussian pulse shape) and the temporal walkoff of the two pulses, we obtained the traces indicated in Fig. 4 for three different assumed DF pulse widths. The cross-correlation traces for the DF FWHM pulses of 25 and 600 fs are for illustration purposes only. The best fit corresponds to a DF FWHM pulse of 310 fs, which is in reasonable agreement with the calculations depicted in Fig. 4. Since the simulations were sensitive to the DF pulse shape, the shape produced by the downconversion simulation associated with Fig. 3 was used. Pulse shapes, such as sech^2, which have lower time–bandwidth products, yielded lower estimates of the DF pulse duration (200–300 fs). For a 310-fs pulse, our time–bandwidth product was 0.7, which was lower than what might be expected given the bandwidth of the signal and idler pulses because of spectral filtering through incomplete phase matching in the DF process as mentioned above.

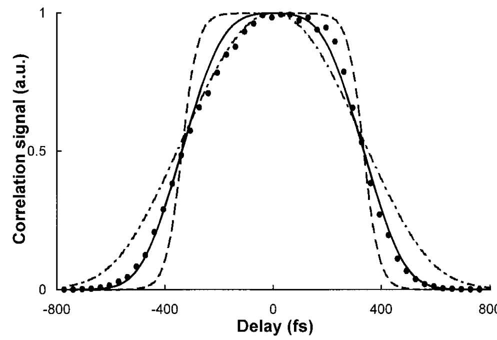

Fig. 4. Normalized cross-correlation data point (●) between the 10.5-μm DF pulses and the 810-nm, 100-fs Ti:sapphire pulses. Negative delay corresponds to the 810-nm pulse arriving at the crystal before the DF pulse. Curves represent results from numerical simulations for various DF pulse widths: dashed curve, DF pulse width of 25 fs; solid curve, pulse width of 310 fs; dash–dot curve, pulse width of 600 fs. The curves corresponding to 25 and 600 fs are for illustration purposes only.

Over the wavelength range of 10–18 μm, the average DF power was measured to be approximately 1 μW as determined after calibration of the HgCdTe detector. For wavelengths longer than 18 μm, the DF power was strongly attenuated by $AgGaSe_2$ absorption, whereas below 10 μm d_{eoe} decreased as θ approached π/2 near a wavelength of 7 μm. Compression of the non-transform-limited signal and idler pulses before mixing would improve output power, albeit by less than 1 order of magnitude. The low average power is also related to the use of single-pass mixing in a thin crystal. Increasing the average power of the DF beam by use of an OPO geometry instead of the single-pass geometry is not feasible with our pump powers. The low gain of the DF mixing process would require high reflectivity mirrors over a wide bandwidth; there are significant material limitations to this. Higher output powers in mid-IR pulses can best be achieved by use of tighter focusing or much higher input peak powers, such as those from an optical parametric amplifier. For example, signal and idler input beams with a repetition rate of 250 kHz and an average power of 100 mW (Ref. 14) would result in average DF powers approaching 1 mW.

4. Conclusions

Limitations on the DF pulses imposed by the use of non-transform-limited pulses are small. In our experiments GVM and GVD determine the final DF pulse width. The GVM between the DF and the signal or idler pulses also restricts the phase-matching bandwidth over most of the 8–15-μm region to limit the spectral content of the DF pulse; at longer wavelengths in which GVM is small, GVD restricts the bandwidth. In a more positive vein, note that, since the optical dispersion of materials is much smaller in the mid-IR than the near-IR or visible regions, we are able to generate light pulses only a few optical cycles in length although the DF pulses have wavelengths of approximately a factor of 10 longer than those of the OPO. The high repetition rate of these pulses, along with the fact that the generating system is primarily solid state, makes this setup relatively easy to use.

We gratefully acknowledge financial assistance from the Natural Sciences and Engineering Research Council of Canada and Technology Ontario.

References and Notes

1. Q. Fu, G. Mak, and H. M. van Driel, "High-power, 62-fs infrared optical parametric oscillator synchronously pumped by a 76-MHz Ti:sapphire laser," Opt. Lett. **17,** 1006–1008 (1992).
2. W. S. Pelouch, P. E. Powers, and C. L. Tang, "Ti:sapphire-pumped, high-repetition-rate femtosecond optical parametric oscillator," Opt. Lett. **17,** 1070–1072 (1992).
3. D. E. Spence, S. Wielandy, C. L. Tang, C. Bosshard, and P. Güntar, "High-repetition-rate femtosecond optical parametric oscillator based on $KNbO_3$," Opt. Lett. **20,** 680–682 (1995).
4. H. M. van Driel, "Synchronously pumped optical parametric oscillators," Appl. Phys. B **60,** 411–420 (1995); see also special issues on optical parametric oscillators in J. Opt. Soc. Am. B (Nov. 1993 and 1995).
5. M. R. X. de Barros, R. S. Miranda, T. M. Jedju, and P. C. Becker, "High-repetition-rate femtosecond mid-infrared pulse generation," Opt. Lett. **20,** 480–482 (1995).
6. J. D. Kafka, M. L. Watts, and J. W. Pieterse, "Infrared pulse generation using a subpicosecond OPO," in *Ultrafast Phenomena IX* P. F. Barbara, W. H. Knox, G. A. Mourou, and A. H. Zewail, eds., Vol. 60 of Springer Series in Chemical Physics (Springer–Verlag, Berlin, 1994), pp. 185–186; J. D. Kafka, M. L. Watts, J. W. Pieterse, and R. L. Herbst, "Mid-infrared pulse generation using a sub-picosecond OPO," Appl. Phys. B **60,** 449–452 (1995).
7. A. Lohner, P. Kruk, and W. W. Rühle, "Generation of 200 femtosecond pulses tunable between 2.5 and 5.5 μm," Appl. Phys. B **59,** 211–213 (1994).
8. R. L. Byer, M. M. Choy, R. L. Herbst, D. S. Chemla, and R. S. Feigelson, "Second harmonic generation and infrared mixing in $AgGaSe_2$," Appl. Phys. Lett. **24,** 65–68 (1974).
9. V. G. Dmitriev, G. G. Gurzadyan, and D. N. Nikogosyan, *Handbook of Nonlinear Optical Crystals* (Springer–Verlag, Berlin, 1991), p. 82.
10. E. C. Cheung, K. Koch, and G. T. Moore, "Silver thiogallate, singly resonant optical parametric oscillator pumped by a continuous-wave mode-locked Nd:YAG laser," Opt. Lett. **19,** 631–633 (1994); C. L. Marquardt, D. G. Cooper, P. A. Budni, M. G. Knights, K. L. Schepler, R. DeDomenico, and G. C. Catella, "Thermal lensing in silver gallium selenide parametric oscillator crystals," Appl. Opt. **33,** 3192–3197 (1994).
11. A. Weiner, "Effect of group velocity mismatch on the measurement of ultrashort optical pulses via second harmonic generation," IEEE J. Quantum Electron. **QE-19,** 1276–1283 (1983); E. Sidick, A. Knoesen, and A. Dienes, "Ultrashort-pulse second-harmonic generation. I. Transform-limited fundamental pulses," J. Opt. Soc. Am. B **12,** 1704–1712 (1995).
12. Ref. 9, p. 84.
13. By tuning the Ti:sapphire laser from 750 to 850 nm, thereby increasing the center wavelengths of both signal and idler pulses in the OPO, we calculate that the temporal walkoff minimum can be shifted between 17.5 and 16.1 μm, thus removing some pulse asymmetry and reducing pulse length by as much as 10%.
14. Coherent Model 9800 optical parametric amplifier product information (Coherent Laser Group, 5100 Patrick Henry Dr., Santa Clara, Calif. 95054).